

Clay-supported graphenes: application to hydrogen storage

Cristina Ruiz-García¹, Javier Pérez-Carvajal¹, Angel Berenguer-Murcia², Margarita Darder¹,

Pilar Aranda¹, Diego Cazorla-Amorós², Eduardo Ruiz-Hitzky^{1,}*

(1) Instituto de Ciencia de Materiales de Madrid, CSIC, Cantoblanco, 28049 Madrid, Spain

(2) Departamento de Química Inorgánica e Instituto Universitario de Materiales, Universidad de Alicante, Apartado 99, E-03080 Alicante, Spain

KEYWORDS: Graphene, clay, sepiolite, montmorillonite, hydrogen storage.

ABSTRACT

The present work refers to clay-graphene nanomaterials prepared by a green way using sucrose (caramel) and two types of natural clays (montmorillonite and sepiolite) as precursors, with the aim to evaluate their potential use in hydrogen storage . The impregnation of the clay substrates by caramel in aqueous media followed by a thermal treatment in absence of oxygen of these clay-caramel intermediates gives rise to graphene-like materials, which remain strongly bound to the silicate support. The nature of the resulting materials was characterized by different techniques such as XRD, Raman spectroscopy and TEM, as well as by adsorption isotherms of N₂, CO₂ and H₂O. These carbon-clay nanocomposites can act as adsorbents for hydrogen storage,

achieving, at 298 K and 20 MPa, over 0.1 wt % of hydrogen adsorption excess related to the total mass of the system and a maximum value close to 0.4 wt % of hydrogen specifically related to the carbon mass. The very high isosteric heat for hydrogen sorption determined from adsorption isotherms at different temperatures (14.5 kJ/mol) fits well with the theoretical values available for hydrogen storage on materials which show a strong stabilization of the H₂ molecule upon adsorption.

1. INTRODUCTION

Clay minerals have been extensively used to develop functional nanomaterials, due to the versatility of these silicates to assemble different types of active species at the nanometric scale (Bergaya F., Then B.K.G., Lagaly G. *Developments in Clay Science Handbook of Clay Science*. **2006**; Ruiz-Hitzky, E.; Aranda, P.; Serratosa, J. M. In *Handbook of Layered Materials*; Auerbach, S. M., Carrado, K. A., Dutta, P., Eds.; Marcel Dekker: New York, 2004; Chapter 3, pp 91-154.). So, for instance, nanoparticles of metal oxides, polymers or biological components can be bound to clays giving rise to a large variety of nanoarchitectures of interest for many applications, such as catalysts (P. Aranda, R. Kun, M. A. Martín-Luengo, S. Letaïef, I. Dékány and E. Ruiz-Hitzky, *Chem. Mater.*, 2008, 20, 84–9; C. Belver, P. Aranda, M. A. Martín-Luengo and E. Ruiz-Hitzky, *Micropor. Mesopor. Mater.*, 2012, 147, 157–162; C. Belver, P. Aranda, E. Ruiz-Hitzky, *J. Mater. Chem. A* (in press) DOI:10.1039/c3ta01686b), magnetic adsorbents (Y. González-Alfaro, P. Aranda, F. M. Fernandes, B. Wicklein, M. Darder and E. Ruiz-Hitzky, *Adv. Mater.*, 2012, 23, 5224–5232), polymer-clay nanocomposites (Ruiz-Hitzky E, Van Meerbeek A. Clay mineral-andorganoclay-polymer

nanocomposite. In: Bergaya F, Theng BKG, Lagaly G, editors. Handbook of clay science development in clay science. Amsterdam: Elsevier; 2006. p. 583–621,), bionanocomposites and biohybrids (Mittal V, editor. Nanocomposites with biodegradable polymers synthesis, properties, and future perspectives. New York: Oxford University Press; 2011; Avérous L, Pollet E, editors. Environmental silicate nano-biocomposites. London: Springer-Verlag; 2012. E. Ruiz-Hitzky, M. Darder, F.M. Fernandes, B. Wicklein, A.C.S. Alcântara, P. Aranda, Prog. Polym. Sci. (in press) <http://dx.doi.org/10.1016/j.progpolymsci.2013.05.004>), etc.

The first attempts to generate carbon-clay materials, presumably in the form of nanostructured graphene-like layers alternating silicate layers in a sandwich type distribution, were carried out by Kyotani and co-workers by intercalation of polyacrylonitrile in layered clays (smectites) followed of thermal treatment in absence of oxygen (Kyotani, T.; Sonobe, N.; Tomita, A., Formation of highly orientated graphite from polyacrylonitrile by using a two-dimensional space between montmorillonite lamellae. *Nature*. 1988, 331 (6154), 331-333. Kyotani, T.; Mori, T.; Tomita, A., formation of a flexible graphite film from poly(acrylonitrile) using a layered clay film as template. *Chem. Mater.* 1994, 6 (11), 2138-2142.). Later on other authors have also reported the formation of carbonaceous materials on clays using diverse carbon sources (Sonobe, N., Kyotani, T. and Tomita, A.(1991) *Carbon*, 29, 61-67; Sandí, G., Winans, R.E. and Carrado, K.A. (1996) *Journal of the Electrochemical Society*, 143, L95-L98.; Sandí, G., Carrado, K. A., Winans, R. E., Johnson, C. S. and Csencsitsc, R. (1999) *Journal of the Electrochemical Society*, 146, 3644-3648; .D Bandosz, T.J., Jagiello, J., Putyera, K. and Schwarz, J.A. (1996) *Chemistry of Materials*, 8, 2023-2029 Duclaux, L., Frackowiak, E.,

Gibinski, T., Benoit, R. and Beguin, F. (2000) Molecular Crystals and Liquid Crystals, 340, 449-454; R. Fernández-Saavedra, P. Aranda, E. Ruiz-Hitzky, Adv. Funct. Mater. 14 (2004) 77-82; P. Aranda, Editors K.A. Carrado, F. Bergaya. The Clay Minerals Society, CMS Workshop Lectures Vol. 14 Ch. 6, 171 (2007); Chantilly, France; P. Aranda, M. Darder, R. Fernández-Saavedra, M. López-Blanco, E. Ruiz-Hitzky, Thin Solids Films 495, 104 (2005)) including ecologically acceptable precursors such as sucrose (Bakandritsos, A.; Steriotis, T.; Petridis, D., High surface area montmorillonite carbon composites and derived carbons. Chem. Mater. 2004, 16 (8), 1551-1559; Bakandritsos, A.; Kouvelos, E.; Steriotis, T.; Petridis, D., Aqueous and gaseous adsorption from montmorillonite-carbon composites and from derived carbons. Langmuir. 2005, 21 (6), 2349-2355.).

We have reported the preparation of graphene-like materials from natural resources like sugar or gelatin supported on clays following an eco-friendly pathway, (Darder, M.; Ruiz-Hitzky, E. R., Caramel-clay nanocomposites. J. Mater. Chem. 2005, 15 (35-36), 3913-3918; Gómez-Avilés A., Darder M., Aranda P., Ruiz-Hitzky E., Functionalized carbon silicates from caramel-sepiolite nanocomposites *Angew. Chem. Int. Ed.* 2007, 46, 923. ; Fernandez-Saavedra, R., Darder M., Gómez Avilés, A., Aranda, P., Ruiz-Hitzky, E., Polymer-clay nanocomposites as precursors of nanostructured carbon materials for electrochemical devices: Templating effect of clays. *J. Nanosci. Nanotech.* 2008, 8 (4), 1741-1750; Gómez-Avilés, A.; Darder, M.; Aranda, P.; Ruiz-Hitzky, E., Multifunctional materials based on graphene-like/sepiolite nanocomposites. *Appl. Clay Sci.* 2010, 47 (3-4), 203-211; Ruiz-Hitzky, E.; Darder, M.; Fernandes, F. M.; Zatile, E.; Javier Palomares, F.J.; Aranda, P., Supported Graphene from Natural Resources: Easy

Preparation and Applications. *Adv. Mater.* **2011**, *23*, 5250-5255) without the requirement of the presence of reducing agents as reported by Tour et al. (Z. Sun, D.K James, J.M. Tour, *J. Phys. Chem. Lett.* **2**, 2425 (2011); M.C. Hermant, *Materials Views*, Sept. 7th, (<http://www.materialsviews.com/sugar-and-spice-and-even-things-not-so-nice-graphene-synthesis/>) (2011).). In addition to the smectite clays, fibrous silicates such as sepiolite and palygorskite appears also as efficient supports for the carbonaceous-clay materials formation. In particular, sepiolite exhibits textural properties and surface activity characteristics (Ruiz-Hitzky, E., Molecular access to intracrystalline tunnels of sepiolite *J. Mater. Chem.* **2001**, *11*, 86-91) able to drive the transformation of diverse organic precursors towards electrical conductive carbons that can be considered graphene-like materials Darder, M.; Ruiz-Hitzky, E. R., Caramel-clay nanocomposites. *J. Mater. Chem.* **2005**, *15* (35-36), 3913-3918; Gómez-Avilés A., Darder M., Aranda P., Ruiz-Hitzky E., Functionalized carbon silicates from caramel-sepiolite nanocomposites *Angew. Chem. Int. Ed.* **2007**, *46*, 923. ; Fernandez-Saavedra, R., Darder M., Gómez Avilés, A., Aranda, P., Ruiz-Hitzky, E., Polymer-clay nanocomposites as precursors of nanostructured carbon materials for electrochemical devices: Templating effect of clays. *J. Nanosci. Nanotech.* **2008**, *8* (4), 1741-1750; Gómez-Avilés, A.; Darder, M.; Aranda, P.; Ruiz-Hitzky, E., Multifunctional materials based on graphene-like/sepiolite nanocomposites. *Appl. Clay Sci.* **2010**, *47* (3-4), 203-211; Ruiz-Hitzky, E.; Darder, M.; Fernandes, F. M.; Zatile, E.; Javier Palomares, F.J.; Aranda, P., Supported Graphene from Natural Resources: Easy Preparation and Applications. *Adv. Mater.* **2011**, *23*, 5250-5255).

Graphene, obtained and studied for the first time by Geim and Novoselov (Novoselov, K. S.; Geim, A. K.; Morozov, S. V.; Jiang, D.; Zhang, Y.; Dubonos, S. V.; Grigorieva, I. V.; Firsov, A. A., Electric field in atomically thin carbon films. *Science*. 2004, 306 (5696), 666-669.), consists of an ideal monolayer of carbon whose excellent electrical conductivity, mechanical and optoelectrical properties, makes it especially attractive for the so-called *advanced applications* in diverse domains (e.g. electrochemical devices such as sensors, batteries or supercapacitors) (S. Guo, S. Dong, Graphene nanosheet: synthesis, molecular engineering, thin film, hybrids, and energy and analytical applications, *Chem. Soc. Rev.*, 2011, 40, 2644; Y.W. Zhu, S. Murali, W.W.Cai, XS. Li, J.W. Suk, J.R. Potts, R.S. Ruoff, *Adv. Mater.* 22, 3906 (2010), L. Ji, Z. Lin, M. Alcoutabi, X. Zhang, *Energy Environ. Sci.* 4, 2682 (2011)). In view of its theoretical elevated specific surface area, calculated as $2630\text{ m}^2/\text{g}$, (S. Stankovich, D. A. Dikin, G. H. B. Dommett, K. M. Kohlhaas, E. J. Zimney, E. A. Stach, R. D. Piner, S T. Nguyen, R. S. Ruoff, *Nature*. 2006, 442, 282), graphene also has potential interest as material for the trapping of gases such as CO_2 and for H_2 storage [A. Ghosh, K.S. Subrahmanyam, K.S. Krishna, S. Datta, A. Govindaraj, S.K Pati, C.N.R Rao, *J. Phys. Chem. C*. **2008**; 112, 15704.; G. Srinivas, Y. Zhu, R. Piner, N. Skipper, M. Ellerby, R. Ruoff, *Carbon*. **2010**, 48, 630; V. Tozzini, V. Pellegrini, *Phys. Chem. Chem. Phys.* **2013**, 15, 80.].

Graphene-based materials can be regarded as potentially useful nanomaterials for hydrogen uptake and storage. In fact, carbon materials (Casa-Lillo, M.; Lamari-Darkrim, F.; Cazorla-Amorós D.; Linares-Solano, A. Hydrogen storage in activated carbons and activated carbon fibers. *J. Phys. Chem. B* 2002, 106, 10930–10934; Jordá-Beneyto, M.; Suárez-García, F.; Lozano-Castelló, D.; Cazorla-Amorós, D. Hydrogen storage on

chemically activated carbons and carbon nanomaterials at high pressures. Carbon 2007, 45, 293–303.), including graphenes (G. Srinivas , Y. Zhu , R. Piner , N. Skipper , M. Ellerby , R. Ruoff , Carbon 2009 , 48 , 630), are able to easily adsorb and desorb hydrogen (C. Ruiz-García, R. Jiménez, J. Pérez-Carvajal, A. Berenguer-Murcia, M., P., D. Cazorla-Amorós, E. Ruiz-Hitzky, "Graphene-clay based nanomaterials for clean energy storage", Sci. Adv. Mater. (submitted) with low enthalpy values, which can be competitive from the practical point of view of their applications compared to metals and MOFs (Hydrogen storage in metal–organic frameworks. L. J. Murray, M. Dincăa, J. R. Long, Chem. Soc. Rev., 2009,38, 1294-1314). For instance, Srinivas *et al.* have reported for graphene materials prepared from graphene oxide reduced with hydrazine a hydrogen adsorption capacity of 0.68 wt% at 77K and 1 bar. (G. Srinivas , Y. Zhu , R. Piner , N. Skipper , M. Ellerby , R. Ruoff , Carbon 2009 , 48 , 630).

The aim of this work is to evaluate the ability of this type of carbon-clay nanocomposite materials, without undergoing removal of the silicate backbone acting as support for the generated graphenes, for adsorbing and desorbing hydrogen gas with views towards exploring their potential application for clean energy storage. Two types of clay substrates, a layered clay (montmorillonite) and a fibrous clay (sepiolite), have been used as support of the resulting graphene-like composites with the aim to determine the influence of their textural characteristics in the final properties of these materials.

2. EXPERIMENTAL DETAILS

2.1. Materials and Reagents

The carbonaceous precursor was liquid caramel Royal (80%) provided by Kraft. Sepiolite clay was supplied by Tolsa, as the commercial product named Pangol® S9 that contains >95% of pure sepiolite. This clay comes from the Vallecas-Vicálvaro deposits in Madrid, Spain. Montmorillonite was supplied by Southern Clay Products (Rockwood Company, Texas) as Cloisite® Na. It is a Wyoming montmorillonite with cation exchange sodium and cationic exchange capacity of ca. 90 meq/100g (Mallakpour S., Dinari M. Preparation and characterization of new organoclays using natural amino acids and Cloisite Na+, Appl. Clay Sci. 2011, 51, 353-359.)

2.2. Preparation Methods

The supported graphene was prepared in a first step by the impregnation of the montmorillonite and sepiolite clays (nominally 4 g), with the liquid caramel in a 2:1 w/w ratio, incorporating 1.2 mL of deionized water per gram of clay. These starting materials were mixed and homogenized by kneading for 20 minutes using a cooking robot Kenwood KM266, giving rise to the hybrid caramel-clay precursors. The precursors were heated under a nitrogen flow using a temperature ramp of 5 °C/min up to a final temperature of 700 °C for the material based on montmorillonite, and 800 °C in the case of sepiolite. The final temperature was maintained for 1 hour for both types of samples. For comparative purposes, the thermal treatment of the starting clays was carried out following an identical way than that adopted for the caramel/clay intermediate composites, i.e. under nitrogen flow until 700 °C for montmorillonite and 800 °C for

sepiolite, at 5 °C/min, and maintaining the final temperature for 1 hour in both types of clays.

2.3. Materials Characterization

Determination of the carbon content was performed by chemical elemental analysis (CHNS PERKIN ELMER 2400 equipment). The X-ray (XRD) diffraction diagrams were obtained on powder samples, using a Bruker D8 Advance diffractometer with $\text{K}\alpha$ Cu radiation equipped with an energy discriminator detector (SOLX), being the voltage and current of the source 40 kV and 30 mA, respectively. These diffractograms were recorded with a goniometer at a speed of 3°/ min between 2 and 60 degrees (2θ). Sample visualization was carried out by transmission electron microscopy in a STEM microscope LEO 910 model operating at 120 kV. Samples were deposited directly on the copper grid covered with carbon from a dilute aqueous suspension of the sample. Samples were placed on a carbon conductive tape without metalizing the surface of the sample. Texture and morphology of samples were observed by FE-SEM using a FEI NOVA NanoSEM 230 equipment without the requirement for samples to be covered with a conductive coating. Raman spectra were obtained using a 532 nm laser (μ Sense-LabC1X Enwave Optronics Raman Confocal equipment). Samples were adhered directly on a carbon tape without any coating on the surface.

Water vapor adsorption-desorption isotherms were measured gravimetrically using an Aquadyne DVS equipment (Quantachrome Instruments). The weight of the samples in powder form was constantly monitored at 25 °C and recorded as the relative humidity

varies between 0 and 95% by using a N₂ stream saturated in water. The adsorbed moisture was expressed as grams of water retained by 100 g of dry sample.

Nitrogen isotherms at 77 K and CO₂ isotherms at 273 K were obtained using an automatic adsorption-desorption equipment (Autosorb-6, Quantachrome). Prior to the adsorption measurements, samples were outgassed at 523 K under vacuum for 4 h. Apparent BET surface areas (S_{BET}) as well as the total micropore volumes (V_p), were calculated from N₂ adsorption isotherms by application of BET and Dubinin-Radushkevich equation, respectively. The volume of micropores smaller than 0.7 nm (V_{up}) is determined from the CO₂ adsorption isotherms at 273 K using Dubinin-Radushkevich equation [Cazorla-Amorós D., Alcañiz-Monge J., Linares-Solano A., Characterization of Activated Carbon Fibers by CO₂ Adsorption. Langmuir 1996; 12(11): 2820–4.].

Hydrogen isotherms were carried out in an automatic volumetric apparatus (Quantachrome device iSorbHP1) designed at the Departamento de Química Inorgánica, Universidad de Alicante laboratory to perform hydrogen isotherms up to 20 MPa. The manifold of the apparatus was kept at 308 K. The sample cell was kept at the adsorption temperature (298K, 323K or 348K) by means of a liquid bath. The manifold volume was calibrated with a standard volume, performing helium isotherms prior to each experiment. In order to ensure that the apparatus was leak-free, hydrogen leak tests were executed at 9 and 15 MPa for 28 h, the resulting leak rate being below 10⁻⁶ s⁻¹. The bulk gas amounts have been calculated by the equation of state of modified Benedict–Webb–Rubin [Zhang C, Lu XS, Gu AZ. How to accurately determine the uptake of hydrogen in carbonaceous materials. Int J Hydrogen Energy

2004;29(12):1271–6] and the cell volume has been calculated taking into account the correction described in the literature [Kiyobayashi, T; Takeshita, HT; Tanaka, H; Takeichi, N; Zuttel, A; Schlapbach, L; Kuriyama, N. Hydrogen adsorption in carbonaceous materials. *J. Alloys Compd.* 2002, 330, 666–669.]. Prior to carrying out the adsorption excess isotherm, the sample was degassed at 423 K under vacuum for 4 h. After that, the sample was located in the sample holder, and then evacuated at 403 K under vacuum for 4 h. Hydrogen and helium gases used in the experiments were 99.9995% pure.

3. RESULTS AND DISCUSSION

3.1. Preparation and characterization of clay-graphene materials

An homoionic sample (Na^+) of montmorillonite layered clay and a rheological degree sepiolite (fibrous clay) have been used as substrates for generation of the supported graphenes. Both classes of clays are able to develop stable colloidal suspensions in aqueous media because in the first case, sodium-exchanged smectites show high tendency to swell in water (H. van Olphen, *An Introduction of Clay Colloid Chemistry*, Intersc. Publish., John Wiley & Sons, N.Y. 1963), and the second one is a commercial clay (Pangel[®]) able to give high viscosity gels in water and other polar media (<http://www.tolsa.com/index.php?idioma=2&seccion=23&contenido=82&padre=31>, 4th June 2013)). These characteristics are relevant for the preparation of homogeneous caramel-clay intermediates used as precursors of the graphene-clay systems, as we used liquid caramel, i.e. with high content in water, as carbon precursor. In a second

step (Fig.1) the intermediate is thermally treated in absence of oxygen at temperatures in the 700-800°C range to produce the transformation of the caramel into carbon as previously reported for sucrose-clay precursors (Darder, M.; Ruiz-Hitzky, E. R., Caramel-clay nanocomposites. *J. Mater. Chem.* **2005**, 15 (35-36), 3913-3918. ; Ruiz-Hitzky, E.; Darder, M.; Fernandes, F. M.; Zatile, E.; Javier Palomares, F.J.; Aranda, P., Supported Graphene from Natural Resources: Easy Preparation and Applications. *Adv. Mater.* **2011**, 23, 5250-5255).

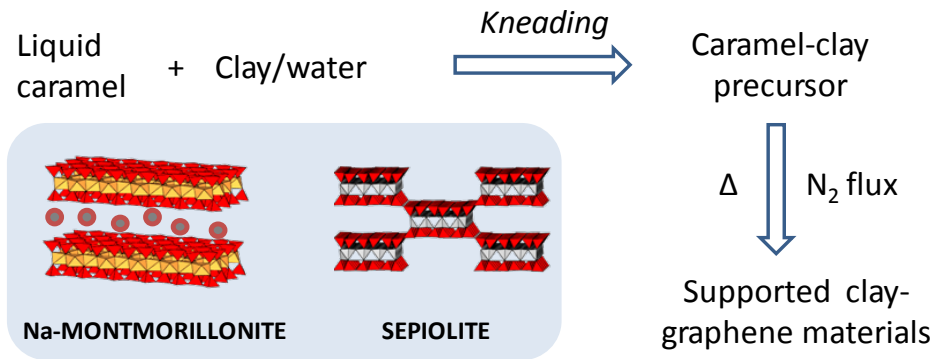


Fig. 1. Scheme of the preparation sequence of clay-graphene materials from liquid caramel and Na-montmorillonite and sepiolite clays.

The resulting materials after heating the intermediates under nitrogen flow at 700°C for the one based on montmorillonite and 800 °C in the case of sepiolite, present a carbon content of ca. 36% (w/w) and 35% (w/w), respectively, as deduced from the CHN chemical analysis. The X-Ray diffractogram of the montmorillonite based materials (Fig. 2) indicates a significant loss of the crystallinity of the starting clay (Fig. 2A) after its assembly with caramel (Fig. 2B), probably due to intercalation-delamination processes, and after the thermal treatment (Fig. 2C), ascribed to a partial clay dehydroxylation. This last process was confirmed by the thermogravimetric results. The basal spacing of the

resulting carbon-montmorillonite materials, deduced from the (001) reflection, is 1.31 nm that corresponds to an intercalated material of ca. 0.4 nm thickness taking into account that the elemental silicate sheet is ca. 0.95 nm thickness. (Darder, M.; Ruiz-Hitzky, E. R., Caramel-clay nanocomposites. *J. Mater. Chem.* 2005, 15 (35-36), 3913-3918.). This value fits well with the formation of a monolayer of carbon atoms between the silicate layers in the same way that reported by Kyotani et al. (Kyotani, T.; Mori, T.; Tomita, A., formation of a flexible graphite film from poly(acrylonitrile) using a layered clay film as template. *Chem. Mater.* 1994, 6 (11), 2138-214; Kyotani, T.; Sonobe, N.; Tomita, A., Formation of highly orientated graphite from polyacrylonitrile by using a two-dimensional space between montmorillonite lamellae. *Nature*. 1988, 331 (6154), 331-333.). In addition to this interlayer carbon, carbon is formed between the clay particles agglomerating them in agreement with FE-SEM observations (Fig. 3A). In the case of the sepiolite-based materials XRD results are not relevant as this type of clay does not exhibit swelling properties being not possible to form intercalated compounds. Therefore, the formed carbon could be located within the sepiolite micropores as well as the external surface of this fibrous clay (Fig. 3B). A similar situation was reported for carbon-sepiolite nanocomposites prepared from acrylonitrile precursors (R. Fernández-Saavedra, P. Aranda, E. Ruiz-Hitzky, *Adv. Funct. Mater.* 14 (2004) 77-82;).

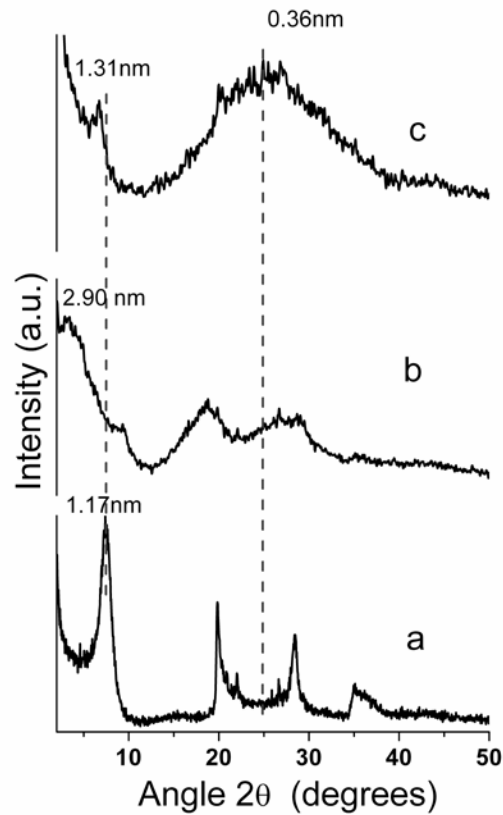


Figure 2. XRD patterns of a) Na-montmorillonite, b) caramel-montmorillonite precursor, and c) carbon-montmorillonite material.

FE-SEM images show the aggregation of sepiolite fibres in the generated carbonaceous material with an homogeneous distribution (Fig. 3B). In the TEM images of this conglomerates (Fig. 4B), it can be easily identify the presence of lamellar particles, quite transparent and with different sizes, which could correspond to graphene-like materials. In the case of montmorillonite based materials it is more difficult to identify the presence of lamellar carbonaceous materials due to the similar morphology of the layered silicate. In this case, it is possible to distinguish particles showing rounded edges, bulky aspect and opaque appearance which can be identified as the montmorillonite clay. In addition

it can be observed lamellar particles, more transparent and shaped with marked corners which can be associated with the presence of the carbonaceous counterpart (Fig. 4A).

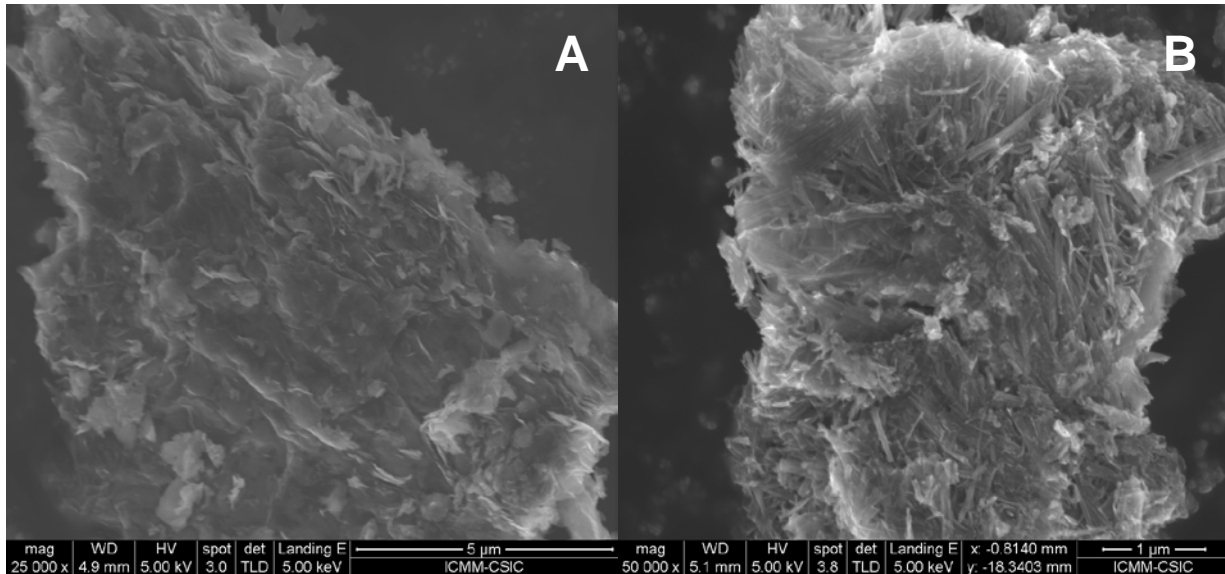


Figure 3. FE-SEM images of carbon-montmorillonite (A) and carbon-sepiolite (B) materials

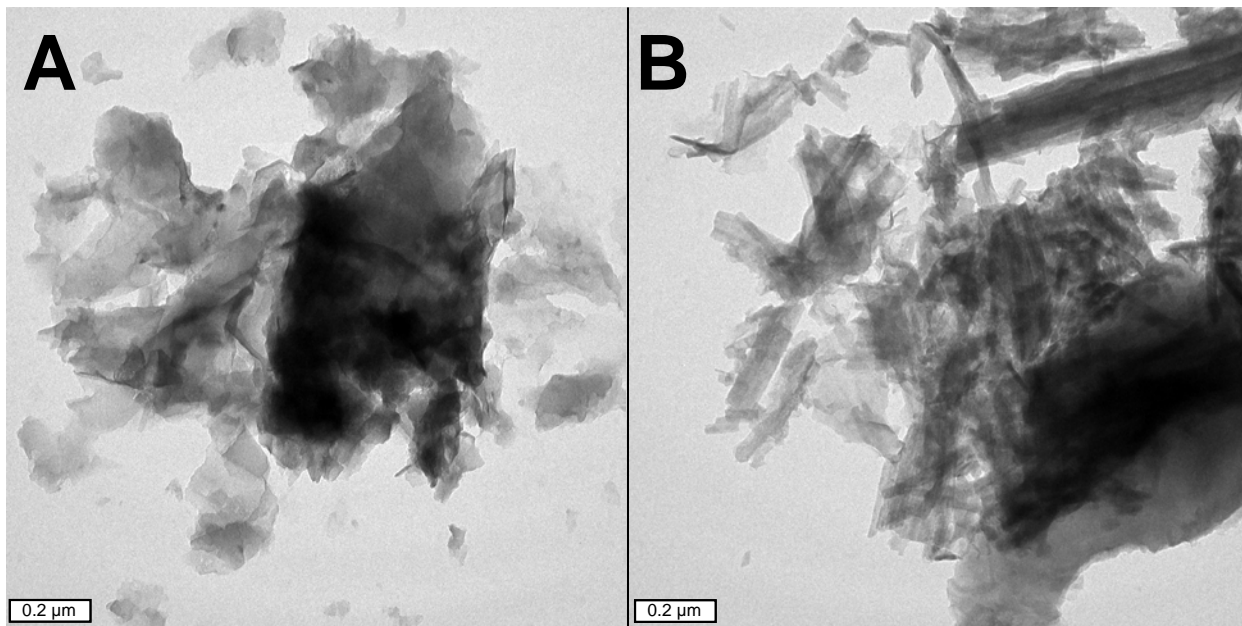


Figure 4. TEM images of carbon-montmorillonite (A) and carbon-sepiolite (B) materials

From the Raman and XPS results it could be inferred that the formed carbon mainly corresponds to graphene-like materials similarly to that reported for carbon-clay materials prepared from sucrose precursor in an alike experimental way (Ruiz-Hitzky, E.; Darder, M.; Fernandes, F. M.; Zatile, E.; Javier Palomares, F.J.; Aranda, P., Supported Graphene from Natural Resources: Easy Preparation and Applications. *Adv. Mater.* **2011**, *23*, 5250-5255). In our case, Raman spectra show the expected signals that affords useful information on the defects (D band), in-plane vibration of sp^2 carbon atoms (G band) as well as the stacking order (2D band) of graphene-like materials (Z. Ni, Y. Wang, T. Yu, Z. Shen, *Nano Res* (2008) *1*: 273-291). The D and G bands, are in our case identified at \sim 1365 and \sim 1600 cm^{-1} and other bands, i.e. 2D, D+G and D' can be recognized after deconvolution with signals centred at around 2730, 2965 and 3200 cm^{-1} .

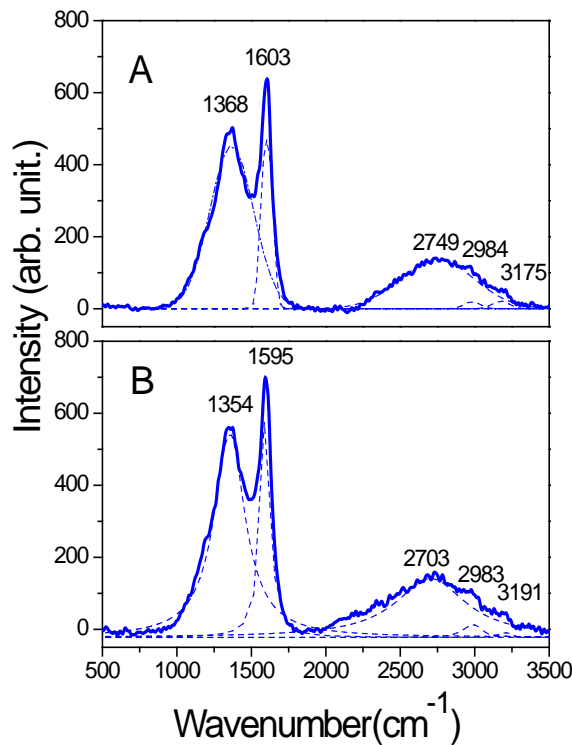


Figure 5. Raman spectra in the region of the typical D and G bands attributed to graphene-like species for carbon-sepiolite (A) and carbon-montmorillonite (B) materials.

3.2. Porous texture of clay-graphene materials

The N₂ adsorption-desorption isotherms obtained at -196°C show similar profiles for both thermally treated clays (Figure 6). Montmorillonite (treated at 700°C) and sepiolite (treated at 800°C) samples show a type IV isotherm according to IUPAC classification with a H3 type hysteresis loop typical of aggregates of plate-like particles (F. Rouquerol, J. Rouquerol, K. Sing, Adsorption by powder and porous solids, Academic Press (1999)). The specific surface area of both thermally treated clays are 16 and 89 m²/g, respectively, exhibiting a strong decrease with respect to the pristine untreated clays (43 and 320 m²/g). The generation of carbon within the clay pores dramatically changes their textural characteristics. In the case of C/MMT (Figure 6a), the amount of nitrogen adsorbed, and consequently the apparent surface area, significantly decrease reaching a value of 4 m²/g (Table 1). The hysteresis loop practically disappears in this sample, which is attributed to the filling of pores by the generated carbon. So, apart from the graphene intercalated between the MMT layers additional carbonaceous material fills the available space within the clay tactoids that was arranged as house-of-cards packing (T.J. Pinnavaia, M.-S. Tzou, S.D. Landau, R.H. Raythatha, *J. Mol. Catal.* 27 (1984) 195–212.; P.F. Luckham, S. Rossi, *Adv. Colloid Interface* 82 (1999) 43–92; C. Belver, P. Aranda, M.A. Martín-Luengo, E. Ruiz-Hitzky, *Micropor. Mesopor. Mater.* 147 (2012) 157–166). Conversely, the N₂ adsorption isotherm of C/SEP (Figure 6b) shows a profile closer to the type IV IUPAC classification with a H4 hysteresis loop (F. Rouquerol, J. Rouquerol, K. Sing, Adsorption by powder and porous solids, Academic

Press (1999)) with a significant increase in the nitrogen adsorbed volume ($S_{BET} = 166 \text{ m}^2/\text{g}$). In this case the generated carbon, located at the external surface of the sepiolite fibers, is accessible to the N_2 adsorbate contributing to the increase of the determined surface area. The observed saturation for the C/SEP sample indicating the absence of macropores can be explained by the complete occupancy of this type of pore volume by the generated carbon.

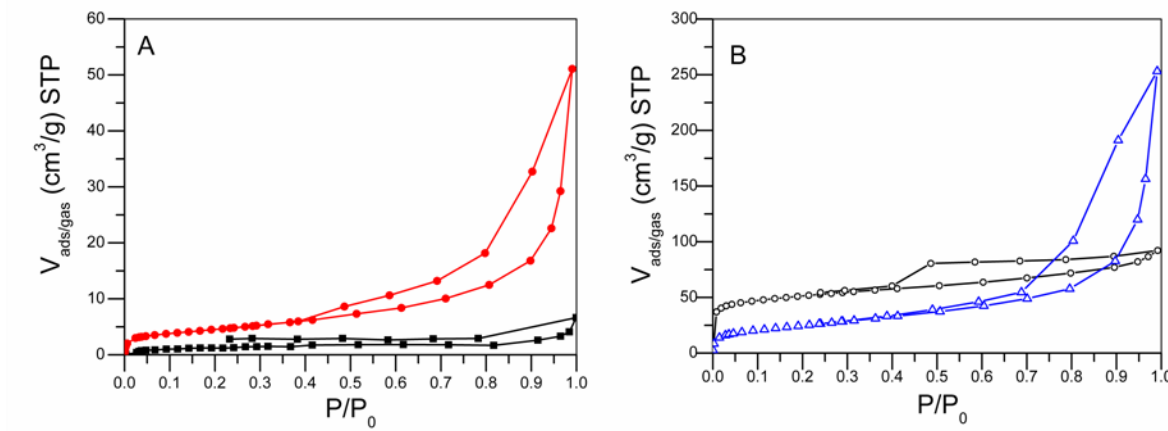


Figure 6. Nitrogen adsorption isotherms at -196°C of A) MMT (treated at 700°C) (●), C/MMT (■), and B) SEP (treated at 800°C) (△) and C/SEP (○) samples

Thermally treated clays do not adsorb CO_2 at 0°C (Figure 7) and the gas adsorption may be mainly attributed to the presence of the formed carbon. This means that the resulting graphene-like materials exhibit quite similar features with the presence of very small pores ($<0.7 \text{ nm}$) which can be of interest, not only as CO_2 containers but also in the hydrogen uptake for energy storage applications.

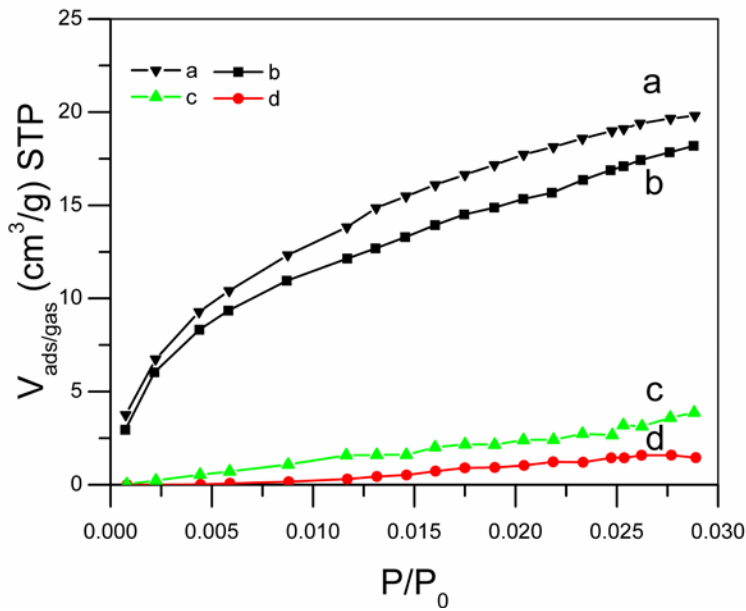


Figure 7. Adsorption isotherms of carbon dioxide at 0°C of a) C/SEP b) C/MMT, c) SEP and d) MMT samples,

Table 1. Textural parameters obtained from the N₂ and CO₂ adsorption isotherms

Sample	S _{BET} (m ² /g)	V _μ (cm ³ /g)	V _{up} (cm ³ /g)
MMT	16	0.007	---
C/MMT	4	0.002	0.06
SEP	89	0.04	---
C/SEP	166	0.08	0.07

* The narrow micropore volumes determined for these samples is negligible

The water vapor sorption isotherms obtained in dynamic mode as reported in the experimental section show different behaviour depending of the type of involved clay (Figure 8). It is observed that the amount of adsorbed water for the thermally treated

clays is lower than for the pristine clays (data not shown). The adsorption on thermally treated MMT is also lower than on SEP, where the calculated values at the maximum adsorption are ca. 11 and 28 % mass change, respectively. The adsorption branch of both isotherms can be classified as type III (S. Brunauer, "The adsorption of gases and vapors", Princeton University Press 1945), which indicates a low affinity between adsorbent and adsorbate. The shape of this curve suggests that water molecules interact with the hydroxyl groups on the clay surface at high relative humidity (RH). The desorption branch of the thermally treated clays changes and can be now classified as type II (S. Brunauer, "The adsorption of gases and vapors", Princeton University Press 1945), which corresponds to the simultaneous presence of strong interaction sites and unspecific adsorption on the surface. In carbon-clay materials the maximum water vapour adsorption values are lower than in the corresponding thermally treated clays, essentially in the case of sepiolite. These values are ca. 6 and 10 % mass change for C/MMT and C/SEP respectively. The observed decrease in water adsorption is in agreement with the hydrophobic character of the generated graphene-like materials covering the clay surface (S. Guo, S. Dong, Graphene nanosheet: synthesis, molecular engineering, thin film, hybrids, and energy and analytical applications, Chem. Soc. Rev, 2011, 40, 2644). The desorption branch of the graphene-like materials shows hysteresis loops more pronounced in C/SEP. As above indicated, these solids present small pores which are particularly accessible to CO₂. Therefore, these hysteresis loops can be related to capillarity effects or ink-bottle porosity during the desorption process. (Moisture sorption practical aspects of isotherm measurement and use, Leonard N. Beii, Theodore P. Labuza 2^aEd 2000 Editors: Amer Assn of Cereal Chemists).

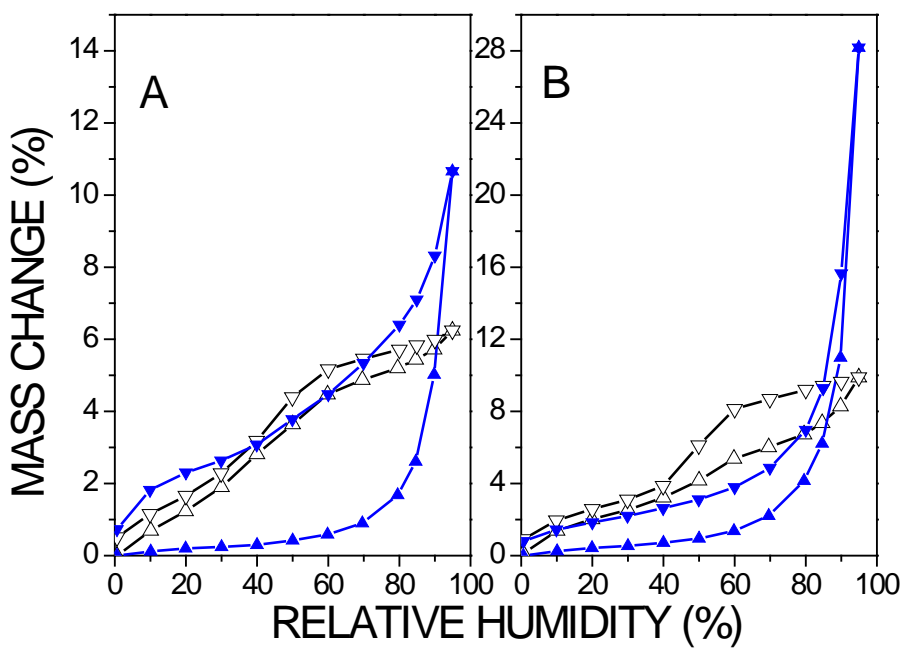


Figure 8. Adsorption-desorption isotherms at 25°C of water on: A) C/MMT sample ($\triangle \nabla$) and montmorillonite treated at 700°C ($\blacktriangle \blacktriangledown$), B) C/SEP sample ($\triangle \nabla$) and sepiolite treated at 800°C ($\blacktriangle \blacktriangledown$)

3.3. Hydrogen uptake by clay-graphene materials

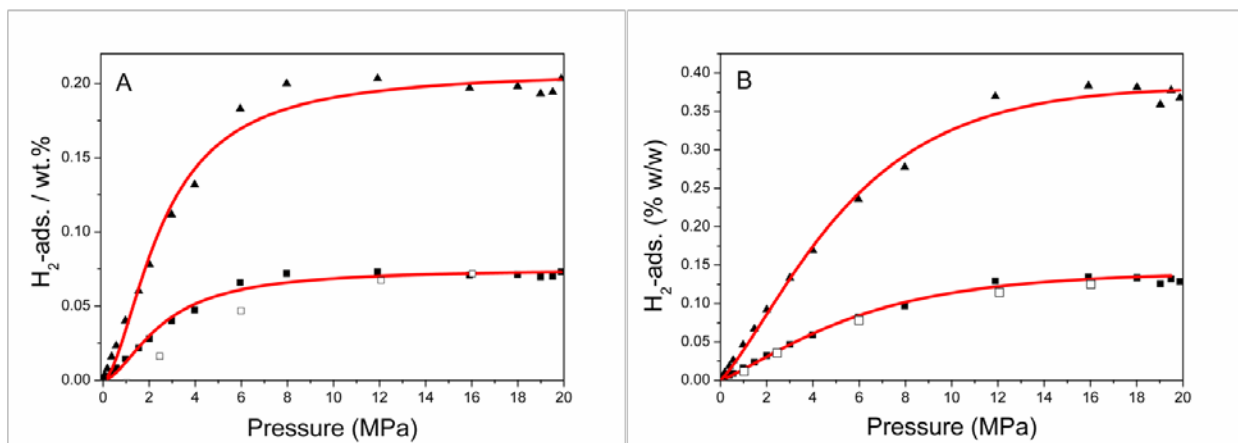


Figure 9. Hydrogen excess adsorption isotherms at 25ºC expressed as a function of the total mass of the sample (adsorption ■, desorption □) and relative only to the carbon mass present in each sample (▲), A) C/MMT and B) C/SEP

Figure 9 shows the H₂ excess adsorption isotherms up to 20 MPa obtained at 25ºC of the clay supported graphene nanomaterials. It should be noted that the clays thermally treated under the same conditions that promote the graphene formation did not show any appreciable H₂ adsorption (values not shown in Fig. 9), which is in accordance to the above mentioned results on CO₂ adsorption. Adsorbed hydrogen on the supported graphene nanomaterials achieve 0.07 and 0.14 % (w/w), respectively for montmorillonite (Figure 9a) and sepiolite (figure 9b), depending on the nature of the clay present in the material.

The hydrogen uptake by the clay-supported graphenes is in the range of graphene materials obtained by chemical exfoliation of graphite (Hydrogen storage performance in palladium-doped graphene/carbon composites, Internat. J. Hydrogen Energ. 38, 3681–3688 (2013)). Thus, it has been reported that these last materials can adsorb ca. 0.2% (w/w) at 15 ºC and 8 MPa. It must be remarked that 65% in weight of the synthetized graphene-clay materials corresponds to a non-adsorbent phase (clay). Therefore, the hydrogen adsorption values, referred to the carbon content of each sample are 0.2 % (w/w) for C/MMT and 0.4 % (w/w) for C/SEP, respectively (Figure 9). This feature suggests that the carbon generated in the presence of sepiolite exhibits a topology that favors the hydrogen adsorption capacity compared to montmorillonite

based materials as well as graphenes from other origin. However, these experimental values are far from the modeling calculation ones or experimental extrapolations (3-4% w/w). (G. Srinivas, Y. Zhu, R. Piner, N. Skipper, M. Ellerby, R. Ruoff, *Carbon*. **2010**, *48*, 630; V.Tozzini, V. Pellegrini, Prospects for hydrogen storage in graphene. *Phys. Chem. Chem. Phys.* **2013**, *15*, 80.)]

The shape of both H₂ adsorption isotherms is different to that displayed by other kind of materials such as high surface area materials or those which present a very narrow porosity [Jorda-Beneyto M, Suarez-Garcia F, Lozano-Castello D, Cazorla-Amoros D, Linares-Solano, A., Hydrogen storage on chemically activated carbons and carbon nanomaterials at high pressures. *Carbon* 2007; *45*(2): 293-303; Kunowsky M., Marco-Lozar J.P., Cazorla-Amorós D., Linares-Solano A., Scale-up activation of carbon fibres for hydrogen storage. *Intl. J. Hydrogen Energy* 2010; *35*(6): 2393-2402]. Regarding to graphene-based materials, few reports on H₂ storage at high pressures can be found in the literature. However, according to those reports [Parambhath V.B., Nagar R., Sethupathi K., Ramaprabhu S., Investigation of spillover mechanism in palladium decorated hydrogen exfoliated functionalized graphene, *J. Phys. Chem. C* 2011; *115*: 15679–15685; Matsuo Y., Ueda S., Konishi K., Marco-Lozar J.P., Lozano-Castelló D., Cazorla-Amorós D., Pillared carbons consisting of silsesquioxane bridged graphene layers for hydrogen storage materials. *Intl. J. Hydrogen Energy*, *2102*; *37*: 10702-10708], hydrogen adsorption on graphene linearly increases with increasing hydrogen pressure with a similar shape to *conventional porous carbons*. The materials here reported seem to have an adsorptive behavior in which saturation is reached at

intermediate H₂ pressures, resulting in a peculiar shape. This particular behavior could be of interest in view to potential applications in gas-storage at low pressures.

The isosteric heat of H₂ adsorption can be calculated by using the Clausius-Clapeyron equation from adsorption isotherms at various temperatures [Li Y.W., Yang R.T., Hydrogen Storage on Platinum Nanoparticles Doped on Superactivated Carbon. J. Phys. Chem. C, 2007; 111: 11086-11094]. So, the sample showing the largest adsorption capacity (C/SEP) was submitted to H₂ adsorption experiments at 323 and 348 K (Figure 10), obtaining a value of 14.5 kJ/mol for low H₂ uptakes. This energy value is substantially higher than that reported for most carbon materials and metal organic frameworks, which are between 4 and 7 kJ/mol. (J. Germain, J.M.J. Fréchet, F. Svec, Nanoporous polymers for Hydrogen storage, Small 2009 5, 10, 1098). The value obtained for the C/SEP sample is in the optimum theoretical range reported for hydrogen storage at room temperature [Bhatia S.K., Myers A.L., Optimum Conditions for Adsorptive Storage. Langmuir, 2006; 22: 1688-1700. J. Germain, J.M.J. Fréchet, F. Svec, Nanoporous polymers for Hydrogen storage, Small 2009 5, 10, 1098]. Recently, Matsuo *et al.* [Matsuo Y., Ueda S., Konishi K., Marco-Lozar J.P., Lozano-Castelló D., Cazorla-Amorós D., Pillared carbons consisting of silsesquioxane bridged graphene layers for hydrogen storage materials. Intl. J. Hydrogen Energy, 2102; 37: 10702-10708] reported the synthesis of pillared carbons consisting of silsesquioxane bridged graphene layers with adsorption heat as high as 11 kJ/mol. The value obtained in that case indicates that hydrogen is greatly stabilized upon adsorption in very narrow pores. This adsorption heat value is close to the calculated physisorption energy ascribed to pores of size close to the H₂ molecular volume [Tozzini V., Pellegrini V., Prospects for

hydrogen storage in graphene. Phys. Chem. Chem. Phys., 2013, 15: 80-89]. This last feature has not been revealed in other carbon based materials, not even graphenes, and points out that in the present carbon-clay materials, the presence of the clay can promote an optimized energy stabilization. To explain the energy stabilization in these carbon-silicate systems, it could be tentatively considered additional physico-chemical effects such as variations on the Van der Waals forces between layers of graphene as reported in graphene adsorbed on silica [M. Boström, B.E. Sernelius, Phys. Rev. A, 2012, 85: 012508].

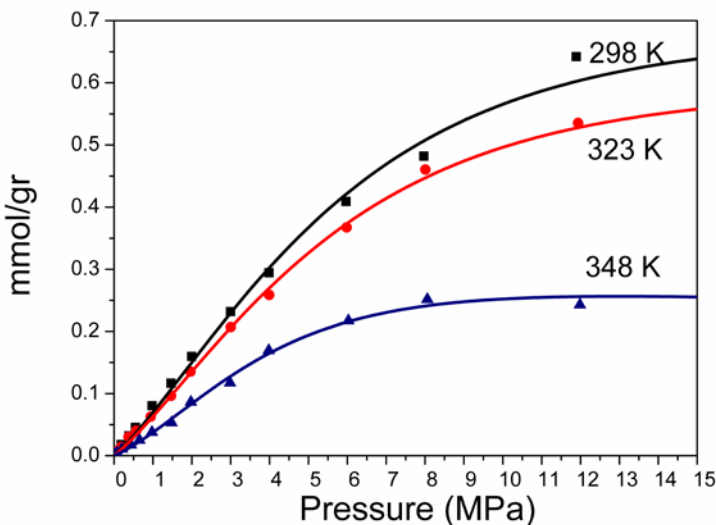


Figure 10. Hydrogen excess adsorption isotherms obtained at different temperatures (25, 50 and 75°C) for the C/SEP sample.

4. CONCLUSIONS

Different topologies and textural behaviors of low-cost and eco-friendly graphene-clay materials results from the combination of silicates of different morphologies (platelets and fibers) with carbon precursors from natural resources (sucrose/caramel). These textural characteristics can be of interest for the adsorption of gases in particular for hydrogen storage in the case of graphene-sepiolite. In spite of these values are not too high compared with other materials (MOFs, nanoporous carbons, metal-hydrides,..) they appear as potentially useful for H₂ storage at room temperature. In fact, very high isosteric heat for hydrogen sorption determined from adsorption isotherms at different temperatures (14.5 kJ/mol) has been measured which fits well with the theoretical values available for hydrogen storage on materials which show a strong stabilization of the H₂ molecule upon adsorption. The presence of the silicate backbone could be profited to incorporate additional functionalization to the carbon-clay systems to enhance adsorption capacity, as for instance by incorporating metal-nanoparticles able to promote hydrogen spill-over effects.

ACKNOWLEDGMENT

Authors thank to the CICYT and FEDER (Spain, projects MAT2012-31759 and CTQ2012-31762) and to the EU COST Action MP1202. The authors also thank Mr. A. Valera, Mr. C. Sebastián and Mr. T. García-Somolinos (ICMM-CSIC) for technical assistance. JP-C thanks a PhD grant (FPI, BES-2010-038410) and AB-M thanks a RyC contract (RyC 2009-03913) from the Spanish Ministerio de Ciencia e Innovación.